JACS
JOURNAL OF THE AMERICAN CHEMICAL SOCIETY
Article
pubs.acs.org/JACS

Realizing Molecular Pixel System for Full-Color Fluorescence Reproduction: RGB-Emitting Molecular Mixture Free from Energy Transfer Crosstalk

Ji Eon Kwon,[†] Sanghyuk Park,[‡] and Soo Young Park*[,†]

[†]Center for Supramolecular Optoelectronic Materials and WCU Hybrid Materials Program, Department of Materials Science and Engineering, Seoul National University, 1 Gwanak-ro, Gwanak-gu, Seoul 151-744, Korea

[‡]Department of Chemistry, Kongju National Univeristy, 56 Gongjudaehak-ro, Gongju, Chungnam 314-701, Korea

Supporting Information

ABSTRACT: A full-color molecular pixel system is realized for the first time using simple mixtures composed of RGB-emitting excited-state intramolecular proton transfer (ESIPT) dyes, each of which has delicately tailored Stokes shift and independent emission capability completely free from energy transfer crosstalk between them. It is demonstrated that the whole range of emission colors enclosed within the RGB color triangle on the CIE 1931 diagram is predictable and conveniently reproducible from the RGB molecular pixels not only in the solution but also in the polymer film. It must be noted that mixing ratios to reproduce the desired color coordinates can be precisely calculated on the basis of additive color theory according to their molecular pixel behavior.

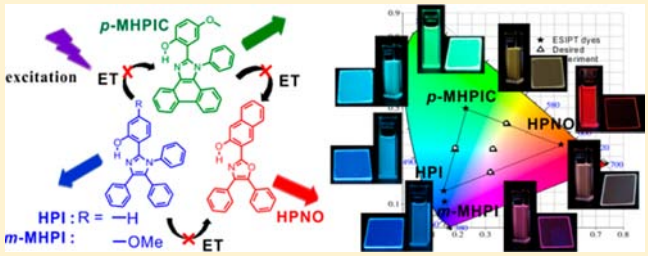

INTRODUCTION

During the past decades, extensive attention has been paid to multicolor luminescent materials due to their application potential in flexible full-color displays,[1−3] in the next-generation lighting sources,[4−6] and in bioimaging agents to decipher multiple biological events simultaneously.[7−10] The method to generate multicolor luminescence is to blend either three primary colors (i.e., red, green, and blue) or two complementary colors (i.e., blue and yellow), while keeping their emission sources independent and free from energy transfer crosstalk through spatial separation of them.[11] In fact, this strategy has been widely used as RGB-emitting pixel system in full-color displays.[12] According to the additive color theory, the entire range of emission colors in the color gamut can be predictable and conveniently reproducible by control of emission intensity ratios between micrometer-sized RGB color pixels. Contrary to bulk pixels, however, reproducing color in a molecular scale by simple mixing of different RGB chromophores is problematic due to the prevalent and unavoidable energy transfer between them.[13] Because the efficiency of energy transfer is exponentially enhanced as the components concentration increases, overwhelmingly dominant emission from the lower band gap components is routinely observed even when they are present in very small amounts.

This energy transfer crosstalk, which is a main obstacle against the realization of "molecular pixel", proceeds through the interaction between an excited-state donor and a ground-state acceptor, irrespective of its actual mechanism (i.e., Förster, Dexter, and trivial). Because the excited state of donor and the ground state of acceptor are highly populated under illumination, the energy transfer between conventional fluorescent dyes cannot be blocked at all. Accordingly, enormous research efforts to achieve multicolor luminescence including white emission have been directed to the elaborate tuning of mixing ratios between energy transferable dyes by trial and error in a specific condition based on gels,[14−19] metal complexes,[20,21] metal−organic frameworks (MOFs),[22,23] self-assembled nanoparticles,[24−27] copolymers,[28−31] polymeric nanoparticles,[32−34] silica nanoparticles,[35−38] and supramolecular polymers,[38−40] instead of completely blocking the energy transfer between different molecules. This approach, however, requires repetitive and time-consuming experiments to check all of emission spectrum for every single mixing ratio of dyes one by one. Needless to say, it is almost impossible to predict and reproduce the emission colors of the mixture precisely in a certain circumstance.

Very recently, unconventional multicolor-emitting molecules showing frustrated energy transfer crosstalk between the emitting centers (i.e., molecular pixel behavior) have been reported by several groups including us, which exploit excited-state intramolecular proton transfer (ESIPT) process.[41−47] ESIPT relies on an enol−keto phototautomerization process of molecules that possess an intramolecular hydrogen bond between a proton-donor (i.e., −OH) and a proton-acceptor

Received: April 29, 2013
Published: July 11, 2013

   dx.doi.org/10.1021/ja404256s | J. Am. Chem. Soc. 2013, 135, 11239−11246

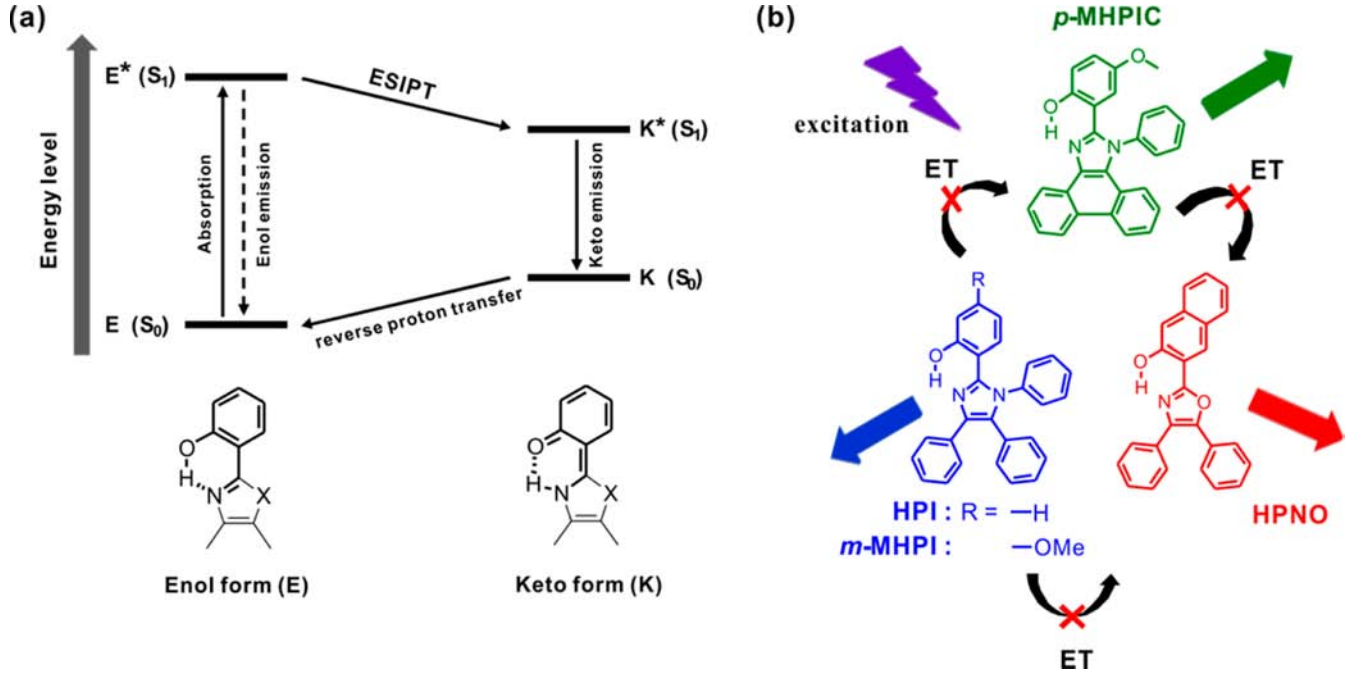

Figure 1. (a) Schematic representation of the ESIPT photocycle. (b) Chemical structures of the ESIPT chromophores used in this study and a schematic illustration of the frustrated energy transfer.

(i.e., −N═) in a five- or a six-membered ring.[48−50] The photoinduced tautomerization transiently generates a keto form (i.e., ═O and −NH−), which typically produces fluorescence with a large Stokes shift (6000−12 000 cm^{-1}). Reverse proton transfer in the ground state from the keto form (K) to the original enol form (E) completes a four-level cyclic proton transfer reaction (E → E* → K* → K → E, see Figure 1a). Because the ground-state K exists only transiently due to the subsequent backward proton transfer, the population of ground-state K as a potential energy acceptor is negligible. As a result, the energy transfer between the ESIPT molecules (i.e., interaction between the K* of donor and K of acceptor) can be totally frustrated.

The frustrated energy transfer between ESIPT chromophores enables them to behave as independent color pixels, even though they are located close to each other within molecular length scale. Even by covalently linking a pair of complementary color-emitting imidazole ESIPT derivatives as subpixels (blue and yellow), we have already demonstrated a two-color "molecular pixel".[42,44] Various photo- and electroluminescence colors from blue through white to yellow could be successfully generated from this molecular pixel emitter by modulating either photoexcitation wavelength or charge carrier balance. For the realistic full-color reproduction, however, we still have to develop a modular system composed of three primary color molecular pixels.

In the present work, we demonstrate a simple and straightforward mixture system, which consists of RGB-emitting molecular pixels harnessing ESIPT for full-color fluorescence reproduction. It is specifically shown that the whole range of emission colors enclosed within the RGB color triangle is precisely predicted and conveniently reproduced from the RGB molecular pixels by adjusting mixing ratios of them, which is based on the exact additive color theory, not only in the solutions but also in the polymer films.

EXPERIMENTAL SECTION

Materials. Materials obtained from commercial suppliers were used without further purification unless otherwise stated. DCM dye was purchased from Sigma-Aldrich. All glassware, syringes, magnetic stirring bars, and needles were thoroughly dried in a convection oven. Reactions were monitored using thin layer chromatography (TLC) with commercial TLC plates (silica gel 60 F254, Merck Co.). Silica gel column chromatography was performed with silica gel 60 (particle size 0.063−0.200 mm, Merck Co.). ^1H and ^{13}C NMR spectra were recorded on a Bruker Avance 300 spectrometer. High-resolution mass (HRMS) spectra were acquired by employing JEOL JMS-600W/JMS-700GC, and elemental analyses were performed on a CE Instrument EA1110 instrument.

Synthesis of *m*-MHPI, 5-Methoxy-2-(1,4,5-triphenyl-1*H*-imidazol-2-yl)phenol. 2-Hydroxy-4-methoxybenzaldehyde (1.00 g, 6.57 mmol) and aniline (0.60 mL, 6.57 mmol) were dissolved in acetic acid (100 mL) and stirred for 1 h at room temperature. Benzil (1.38 g, 6.57 mmol) and ammonium acetate (3.55 g, 46.00 mmol) were added subsequently. The mixture was heated at 120 °C overnight. After termination of the reaction, the dark solution was poured into copious amounts of water. After neutralization, the mixture was filtered and washed with water. Reprecipitation in methanol from dichloromethane solution afforded white powder (1.64 g, yield = 60%). ^1H NMR (300 MHz, $CDCl_3$, δ): 13.68 (s, 1H), 7.53 (dd, J = 8.1, 1.4 Hz, 2H), 7.42−7.32 (m, 3H), 7.30−7.10 (m, 10H), 6.61 (d, J = 2.6 Hz, 1H), 6.42 (d, J = 8.9 Hz, 1H), 6.04 (dd, J = 8.9, 2.6 Hz, 1H), 3.76 (s, 3H). ^{13}C NMR (75 MHz, $CDCl_3$, δ): 161.17, 160.56, 145.51, 137.40, 134.99, 133.41, 131.56, 130.17, 130.02, 129.77, 129.31, 128.98, 128.62, 128.53, 128.44, 127.08, 106.51, 105.45, 102.10, 55.38. HRMS (FAB+, m/z): $[M + H]^+$ calcd for $C_{28}H_{23}N_2O_2$, 419.1760; found, 419.1761. Anal. Calcd for $C_{28}H_{22}N_2O_2$: C, 80.36; H, 5.30; N, 6.69. Found: C, 80.36; H, 5.39; N, 6.65.

Synthesis of *p*-MHPIC, 4-Methoxy-2-(1-phenyl-1*H*-phenanthro[9,10-*d*]imidazol-2-yl)phenol. 2-Hydroxy-5-methoxybenzaldehyde (1.07 g, 7.00 mmol) and aniline (0.64 mL, 7.00 mmol) were dissolved in acetic acid (100 mL) and stirred for 1 h at room temperature. 9,10-Phenanthrenequinone (1.46 g, 7.00 mmol) and ammonium acetate (3.78 g, 49.00 mmol) were added subsequently. The mixture was heated at 120 °C overnight. After termination of the reaction, the dark solution was poured into copious amounts of water.

dx.doi.org/10.1021/ja404256s | J. Am. Chem. Soc. 2013, 135, 11239−11246

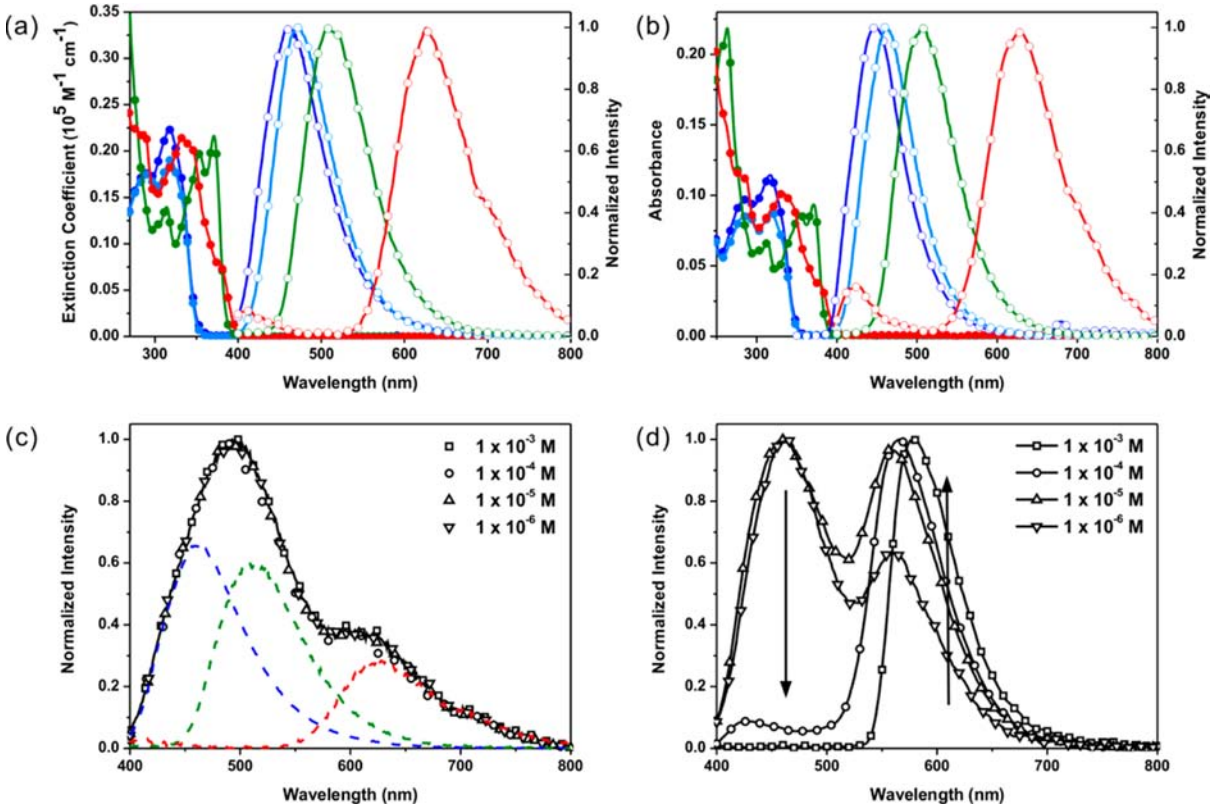

Figure 2. Optical properties of the ESIPT molecules. Absorption (filled circles) and normalized photoluminescence (empty circles) spectra of *m*-MHPI (blue), HPI (sky blue), *p*-MHPIC (green), and HPNO (red) (a) in solution ($CHCl_3$, $c = 1 \times 10^{-5}$ M) and (b) in dye-doped PMMA films (c = 1 wt %) at room temperature. The excitation wavelength was 330 nm for the solutions and 340 nm for the films, respectively. (c) Normalized emission spectra of the ESIPT dye ternary mixtures with molar ratios of *m*-MHPI:*p*-MHPIC:HPNO = 1:3:5 in chloroform solution at different concentrations (1×10^{-6} to 1×10^{-3} M). The dashed lines indicate the estimated spectra of the mixture (black) and the corresponding dye component: *m*-MHPI (blue), *p*-MHPIC (green), and HPNO (red), respectively. The excitation wavelength was 330 nm. (d) Normalized emission spectra of the binary mixture with molar ratios of *m*-MHPI/DCM = 1:1 in chloroform solution at different concentrations (1×10^{-6} to 1×10^{-3} M). Arrows indicate direction of spectral changes with increasing dye concentrations. The excitation wavelength was 320 nm.

After neutralization, the mixture was filtered and washed with water. The organic compounds were reprecipitated in methanol from dichloromethane solution, which was dried over anhydrous $MgSO_4$ and concentrated. Silica gel column purification with EtOAc:$CHCl_3$:*n*-hexane (1:10:50, v/v/v) gave a white powder (1.24 g, yield = 45%). ^{1}H NMR (300 MHz, $CDCl_3$, δ): 13.32 (s, 1H), 8.78 (d, J = 8.3 Hz, 1H), 8.71 (d, J = 8.2 Hz, 2H), 7.83−7.60 (m, 7H), 7.53 (t, J = 7.4 Hz, 1H), 7.31−7.21 (m, 1H), 7.06 (dd, J = 8.5, 4.2 Hz, 2H), 6.82 (dd, J = 8.9, 2.9 Hz, 1H), 6.34 (d, J = 2.9 Hz, 1H), 3.29 (s, 3H). ^{13}C NMR (75 MHz, $CDCl_3$, δ): 153.61, 151.33, 148.41, 139.48, 134.72, 131.12, 130.77, 129.69, 129.47, 128.63, 127.68, 127.21, 126.70, 126.25, 126.00, 125.45, 124.38, 123.38, 122.77, 121.01, 118.95, 118.83, 112.65, 109.71, 55.32. HRMS (FAB+, m/z): $[M + H]^+$ calcd for $C_{28}H_{21}N_2O_2$, 417.1603; found, 417.1606. Anal. Calcd for $C_{28}H_{20}N_2O_2$: C, 80.75; H, 4.84; N, 6.73. Found: C, 80.77; H, 4.80; N, 6.73.

Measurements. UV−vis absorption spectra were collected on a Shimadzu UV-1650PC spectrophotometer at room temperature. Fluorescence spectra were obtained by using a Varian Cary Eclipse fluorescence spectrophotometer. The photoluminescence quantum efficiencies ($\Phi_{r,\,PL}$) in solution were obtained using quinine sulfate in 1.0 N sulfuric acid as a reference. On the other hand, the $\Phi_{ab,PL}$ values in thin films on a quartz plate were measured using a 3.2-in. integrating sphere equipped on a QM-40 spectrophotometer (Photon Technology International, Canada). Time-resolved fluorescence lifetime experiments were performed through the time-correlated single photon counting (TCSPC) methods by using a FluoTime 200 instrument (Picoquant, Germany). A 342 nm pulsed LED with repetition rate of 10 MHz was used as an excitation source. Fluorescence decay profiles were analyzed by FluoFit Pro software, using exponential fitting models through deconvolution employing instrumental response functions (IRF).

Calculations. All density functional theory (DFT) calculations were carried out in the gas phase using the Gaussian 09 quantum-chemical package.[51] The geometry optimizations for the ground state of imidazole and oxazole derivatives were performed using B3LYP functionals with 6-31G(d,p) basis set.[52] Vibration frequency calculations at the same level were performed for the obtained structures to confirm the global minimum.

■ RESULTS AND DISCUSSION

To construct a molecular pixel system for full-color reproduction, three primary color-emitting ESIPT chromophores having suitable Commission Internationale de l'Eclairage (CIE) chromaticity coordinate as well as high fluorescence quantum yield are ideally desirable. The hydroxy-substituted tetraphenylimidazole derivatives are typical ESIPT molecules, which emit strong fluorescence not merely in the solution but more intensely in the solid state. It is rationalized that the steric crowding of the four phenyl rings prevents tight stacking of the active chromophores, thereby maintaining appropriate intermolecular distances to suppress intermolecular nonradiative decay pathways.[53−58] A highly efficient amplified spontaneous emission as well as organic light-emitting diodes (OLEDs) was successfully demonstrated with the ESIPT-active imidazole molecules incorporating multifunctional substituents.[42,44,53,54] Although we have already developed and demonstrated a series

dx.doi.org/10.1021/ja404256s | J. Am. Chem. Soc. 2013, 135, 11239−11246

Table 1. Photophysical Properties of the Imidazole Derivatives in $CHCl_3$ Solution and PMMA Doped Thin Films

	solution[a]				film[b]			fluorescence lifetime[e]		
	$\lambda_{max,abs}$ (nm)	ε (L mol^{-1} cm^{-1})	$\lambda_{max,em}$ (nm)	$\Phi_{r,PL}$[c]	$\lambda_{max,abs}$ (nm)	$\lambda_{max,em}$ (nm)	$\Phi_{ab,PL}$[d]	τ_1 (ns)	τ_2 (ns)	τ_{avg}(ns)
m-MHPI	317	2.23×10^4	461	0.062	317	447	0.27	2.14 (71.9%)	3.07 (28.1%)	2.40
HPI	319	1.91×10^4	472	0.15	318	462	0.37	2.42 (24.7%)	3.93 (75.3%)	3.55
p-MHPIC	371	2.17×10^4	513	0.032	371	506	0.44	1.59 (25.4%)	5.04 (74.6%)	4.16
HPNO	333	2.15×10^4	628	0.0057	332	422, 623	0.014	0.63 (69.9%)	1.56 (30.1%)	0.91

[a]10 μM in $CHCl_3$. [b]1 wt % of dye doped in PMMA. [c]The relative PL quantum yields were measured using quinine sulfate as a reference. [d]The absolute PL quantum yields were measured using an integrating sphere with QM40 spectrophotometer. [e]The fluorescence lifetime values of the films were measured at 440, 460, 520, and 620 nm for *m*-MHPI, HPI, *p*-MHPIC, and HPNO, respectively.

of nine imidazole ESIPT derivatives whose emission wavelength was widely tuned from 470 to 630 nm,[59] they still lack one exhibiting green K* emission (500 nm < λ_{max} < 550 nm). In addition, the highest energy emitting fluorophore, 2-(1,4,5-triphenyl-1*H*-imidazol-2-yl)phenol (HPI, λ_{max} = 472 nm, Figures 1b and 2a) in the series does not show deep blue emission but only sky blue emission, which is rather insufficient for the full-color reproduction.

Therefore, two imidazole-based ESIPT derivatives were newly designed and synthesized in this work for the blue and green emitting molecular pixels by introducing a donor substituent such as methoxy group into the phenol ring of HPI. As previously reported by us,[42] DFT calculation results show that π-electrons of both the highest occupied and the lowest unoccupied molecular orbitals (HOMO and LUMO) are extensively delocalized over the whole molecule in the case of enol form of HPI (see Supporting Information Figure S1). Yet, the occurrence of proton transfer, forming a keto form, brings about π-electron deficiency at a specific position especially in the phenol ring. In the case of keto form of HPI, π-electron density of the HOMO at *meta*-position to the ketone group is lower than the other positions. In contrast, π-electron density of the LUMO is deficient at *para*-position to the ketone group of the keto form of HPI. It is, therefore, expected that adding a methoxy group at the *meta*-position should raise the LUMO energy of the keto form while hardly affecting the HOMO level, to give an overall hypsochromic shift of the K* emission. Conversely, a similar substitution at the *para*-position should raise only the HOMO energy of the keto form, resulting in a bathochromic shift of the K* emission (see Supporting Information Figure S2).

According to the classic lophine synthesis,[60] both *m*-MHPI and *p*-MHPIC (see Figure 1b and Supporting Information Scheme S1) were synthesized in good yield by the reaction with aniline and the corresponding methoxy-substituted salicylaldehydes, respectively. To induce sufficient bathochromic shift for green emission, the extended conjugation length strategy[59] was additionally implemented by the use of 9,10-phenanthrenequinone instead of benzil in *p*-MHPIC synthesis. HPNO, the lowest energy emitting fluorophore in the imidazole series,[59] was selected as a red emitting molecular pixel and synthesized as described elsewhere.[61] All new synthesized materials are fully characterized by ^{1}H NMR, ^{13}C NMR, HRMS, and elemental analysis (see Experimental Section).

Steady-state UV−vis absorption and normalized fluorescence emission spectra of the synthesized molecules in chloroform solution and dye-doped polymethyl methacrylate (PMMA) films are shown in Figure 2a and b, respectively. The details including photoluminescence quantum yields (Φ_{PL}) and fluorescence lifetimes (τ) are also summarized in Table 1. As we intended, *m*-MHPI and *p*-MHPIC showed blue (λ_{max} = 461 nm) and green (λ_{max} = 513 nm) fluorescence emission in the solution, which were blue- (11 nm) and red-shifted (41 nm) as compared to that of nonsubstituted HPI (λ_{max} = 472 nm), respectively. HPNO exhibited red (λ_{max} = 628 nm) K* emission with a very weak E* emission band at around 410 nm in the solution. The relative quantum yields ($\Phi_{r,PL}$) of the solutions are 0.062, 0.032, and 0.0057 for the blue (*m*-MHPI), green (*p*-MHPIC), and red (HPNO) emissions, respectively.

On the other hand, a slight hypsochromic shift of the emission was observed in the imidazole dye-doped PMMA films, whereas their absorption was almost identical to those in the solution. Nevertheless, the imidazole molecules still fluoresce three primary RGB colors in the polymer films, respectively. Furthermore, it is noteworthy that these RGB imidazole derivatives exhibited a large Stokes shifted emission (>130 nm) between 440 and 630 nm originating from their respective keto tautomers, while their absorption spectra were all localized within UV region, leading to almost no spectral overlap between their absorption and emission bands.

To identify a given set of chromophores as molecular pixels, the emission spectrum of individual chromophore molecule should be unaffected by the presence of other chromophores when they are mixed together even to the very high concentrations. To confirm the independent emission, three sets of ternary mixture solutions were prepared in molar ratios of *m*-MHPI:*p*-MHPIC:HPNO = 5:3:1, 1:1:1, and 1:3:5, respectively, at various total chromophore concentrations from 1 μM to 1 mM. As expected for the molecular pixels showing frustrated energy transfer crosstalk, the measured emission spectra of the mixture solutions could be precisely estimated by simply adding the emission spectra of individual components weighted to their mixing ratios (see the scattered symbols and dashed lines in Figure 2c and Figure S3 in the Supporting Information). It should be noted that spectral shape of a given mixture solution is independent of its total chromophore concentration, providing unambiguous evidence for frustrated energy transfer between the emitting components in the mixture solutions. The main principle and working mechanism of frustrated energy transfer between ESIPT imidazole species have been described in full detail in our earlier publication.[42]

On the contrary, as total chromophore concentration increased, a significant red-shift of emission was observed from binary mixture solutions containing *m*-MHPI and a well-known conventional red emitter ($\lambda_{max,abs}$ = 471 nm and $\lambda_{max,PL}$ = 565 nm in 10 μm $CHCl_3$ solution) 4-(dicyanomethylene)-2-methyl-6-(4-dimethylaminostyryl)-4*H*-pyran (DCM, see Supporting Information Figure S4).[62] Above 0.1 mM of total concentration, the blue emission from *m*-MHPI at around 460 nm was almost completely quenched, whereas the red emission from DCM at around 580 nm was noticeably enhanced (see

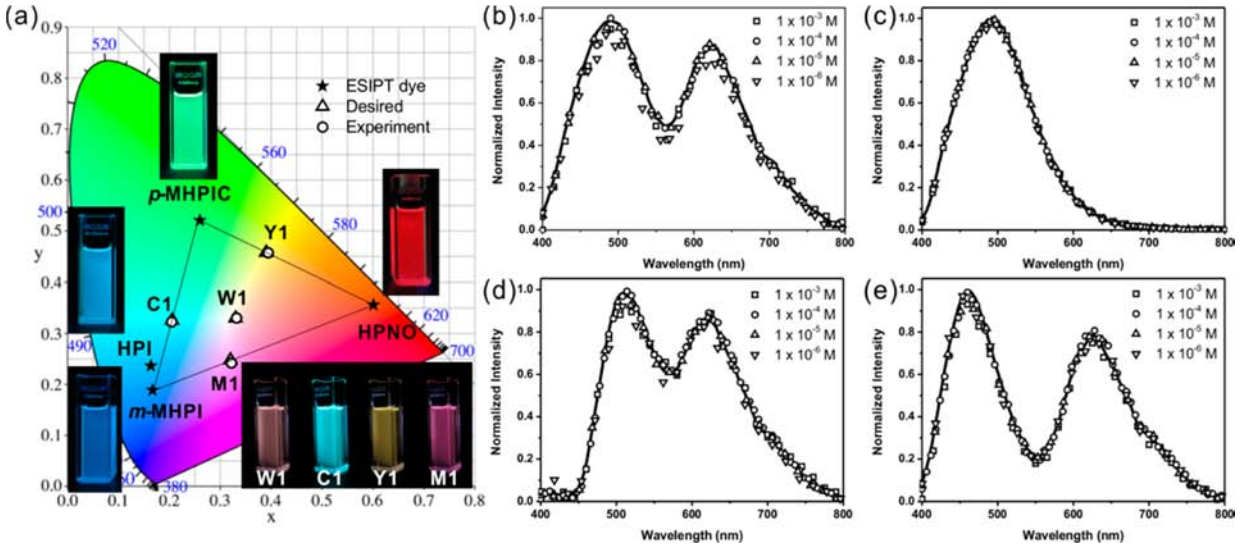

Figure 3. (a) Emission color coordinates of the solution mixtures in the CIE 1931 chromaticity diagram: individual ESIPT dyes (★, *m*-MHPI, HPI, *p*-MHPIC, and HPNO), desired values (△), and experimentally obtained values of the mixtures (○, W1, C1, Y1, and M1). The inset shows photographs of the individual ESIPT dyes and the corresponding mixtures under 330 nm UV light. Normalized emission spectra of the corresponding solution mixtures: (b) W1, (c) C1, (d) Y1, (e) M1 at different concentrations (1×10^{-6} to 1×10^{-3} M). The black solid lines indicate the expected spectra of the mixtures. The excitation wavelength was 330 nm.

Table 2. Mixing Ratios and the CIE Chromaticity Coordinates of the Mixture Solutions and the PMMA Doped Mixture Films

name		mixing ratio[a]			chromaticity coordinates (*x*, *y*)	
		b	*g*	*r*	desired	obtained
solution	W1	0.077	0.19	1.0	0.330, 0.330	0.332, 0.330
	C1	0.37	1.0	0	0.205, 0.326	0.204, 0.323
	Y1	0	0.37	1.0	0.390, 0.458	0.394, 0.457
	M1	0.11	0	1.0	0.320, 0.248	0.322, 0.242
film	W2	0.019	0.015	1.0	0.330, 0.330	0.327, 0.332
	C2	1.0	0.91	0	0.190, 0.329	0.192, 0.336
	Y2	0	0.023	1.0	0.380, 0.434	0.376, 0.436
	M2	0.031	0	1.0	0.320, 0.233	0.318, 0.234

[a]Mixing ratios of *b*:*g*:*r* are *m*-MHPI:*p*-MHPIC:HPNO in moles for the mixture solutions and HPI:*p*-MHPIC:HPNO in weight for the mixture films, respectively.

Figure 2d). This is attributed to efficient energy transfer from *m*-MHPI to DCM because the emission of *m*-MHPI and the absorption of DCM have significant overlap (spectral overlap integral, $J(\lambda) = 1.25 \times 10^{15}$ nm^4 M^{-1} cm^{-1}).[63] It means that conventional DCM molecules are very good energy acceptors for K* emission of *m*-MHPI in the mixed solutions.

We evaluated molecular pixel behavior of the synthesized ESIPT molecules by reproducing colors in the CIE 1931 *XYZ* color space and the *xy* chromaticity diagram.[11] The chromaticity coordinates (*x*, *y*) of the imidazole molecules in the solution are (0.167, 0.189) for *m*-MHPI, (0.260, 0.521) for *p*-MHPIC, and (0.601, 0.356) for HPNO, respectively. As shown in Figure 3a, the chromaticity coordinates of *m*-MHPI, *p*-MHPIC, and HPNO correspond to blue, green, and red colors of the CIE 1931 chromaticity diagram, respectively, and form a color triangle called gamut that is the range of colors that can be generated from additive combination of the three emissions at its corners. According to Grassmann's law, a mixing ratio *b*:*g*:*r* for reproducing a certain desired color having chromaticity coordinate of (*x*, *y*) can be easily calculated by simple mathematical operations if the mixing components have additive property (see the Supporting Information for the operation details).[11] A white color (W1) as well as secondary colors including cyan (C1), yellow (Y1), and magenta (M1) within the triangle were selected to reproduce as representative examples (see Figure 3a). A molar mixing ratio of *m*-MHPI:*p*-MHPIC:HPNO = 0.077:0.19:1.0 was obtained to reproduce an ideal white color W1 having chromaticity coordinates of (0.330, 0.330). In practice, mixing the three imidazole molecular pixels produced a white emission with chromaticity coordinates of (0.332, 0.330), which is almost identical to the desired color. In the same way, the other secondary colors were successfully reproduced with reasonable accuracy as summarized in Table 2. It is worth noting that the spectral shape and the chromaticity coordinates of the reproduced colors did not change at all, while total chromophore concentration varied from 1 μM to 1 mM (see Figure 3b–e).

Importantly, the molecular pixel system functioned not only in the solution but also in the solid thin films, which is crucial for the real application. Interestingly, the imidazole molecular pixels showed remarkably enhanced emission as compared to that in the solution due to the bulky phenyl rings (see Table 1 and vide supra). The absolute photoluminescence quantum yields ($\Phi_{ab,PL}$) of the films were 0.27, 0.44, and 0.014 for *m*-MHPI, *p*-MHPIC, and HPNO, respectively. However, a slight hypsochromic shift in the emission of the films as compared to

dx.doi.org/10.1021/ja404256s | J. Am. Chem. Soc. 2013, 135, 11239–11246

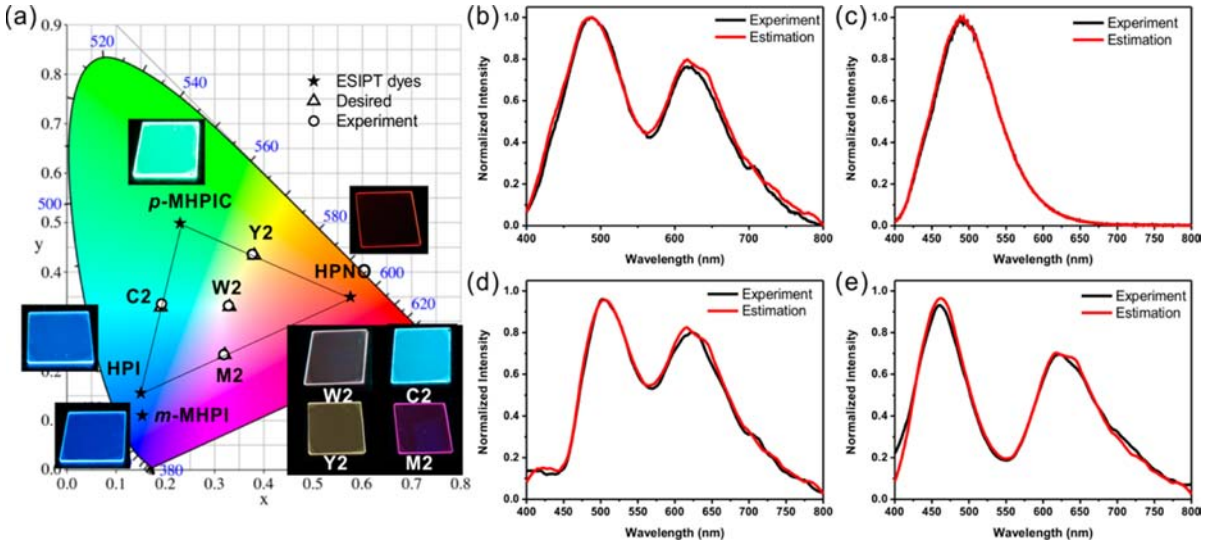

Figure 4. (a) Emission color coordinates of the ESIPT dye-doped PMMA film mixtures (total c = 1 wt %) in the CIE 1931 chromaticity diagram: individual ESIPT dyes (★, *m*-MHPI, HPI, *p*-MHPIC, and HPNO), desired values (△), and experimentally obtained values of the mixtures (○, W2, C2, Y2, and M2). The inset shows the photographs of the individual ESIPT dyes and the corresponding mixtures under 340 nm UV light. Normalized emission spectra of the corresponding film mixtures: (b) W2, (c) C2, (d) Y2, (e) M2. The excitation wavelength was 340 nm.

that in solution (vide supra) resulted in a small spectral overlap between the emission of *m*-MHPI and the absorption of *p*-MHPIC as well as that of HPNO (see Supporting Information Figure S5). It means that ground-state E form of both *p*-MHPIC and HPNO turned into a potential energy acceptor for the K* emission of *m*-MHPI in the film state. As a result, despite fairy small overlap ($J(\lambda) \approx 1 \times 10^{12}$ nm^4 M^{-1} cm^{-1}, see the Supporting Information), it was observed that the blue emission from *m*-MHPI at around 440 nm was significantly decreased, while the green and red emissions from *p*-MHPIC and HPNO at around 500 and 610 nm were non-negligibly enhanced due to partial energy transfer from *m*-MHPI to *p*-MHPIC and HPNO in their simple binary mixture films (*m*-MHPI:*p*-MHPIC and *m*-MHPI:HPNO = 1:1 in weight), respectively (see Supporting Information Figure S6).

Fortunately, however, such inappropriate blue molecular pixel for full-color reproduction in the film state could be replaced by HPI. Because of the hypsochromic shift of the emission in the PMMA film, the HPI-doped film showed appropriately blue-shifted emission color in the CIE diagram, which made no spectral overlap with *p*-MHPIC and HPNO (see Figure 4a and Supporting Information Figure S5). The chromaticity coordinates (x, y) of the imidazole-doped films are (0.150, 0.156) for HPI, (0.229, 0.499) for *p*-MHPIC, and (0.575, 0.350) for HPNO, respectively. Through the exact same procedures as in the solution, representative colors including a white (W2), cyan (C2), yellow (Y2), and magenta (M2) within the gamut were successfully reproduced in the films (see Figure 4a and Table 2). Moreover, it should be noted that all of the reproduced emission spectra were exactly matched with predicted ones, which unambiguously confirmed their molecular pixel behavior (see Figure 4b–e).

Finally, fluorescence lifetime measurements could underpin that the molecular pixel behavior of the films is attributed to the frustrated energy transfer between the ESIPT molecules. As summarized in Table 1, all of the four imidazole molecules exhibited biexponential decay in PMMA films (see Supporting Information Figures S7–10 for decay profiles). To check fluorescence lifetime changes, five different binary mixture films were prepared in 1:1 weight ratio: (1) HPI and *p*-MHPIC (HP11); (2) HPI and HPNO (HO11); (3) *p*-MHPIC and HPNO (PO11); (4) *m*-MHPI and *p*-MHPIC (MP11); and (5) *m*-MHPI and HPNO (MO11), respectively. In the conventional resonant energy transfer system, the presence of acceptor molecules shortens the fluorescence lifetime of donor molecules.[13] In contrast, HPI being an ineffective energy donor exhibited almost unaltered decay profiles (χ^2 = 1.04) with lifetimes of 2.42 ns (33.6%) and 4.02 ns (66.4%) in the HO11 film when monitored at 500 nm. Similarly, despite the presence of excess amount of HPNO, *p*-MHPIC did not show any significant lifetime changes in the PO11 film with time constant of 1.63 ns (26.6%) and 5.00 ns (73.4%) when monitored at 520 nm (χ^2 = 1.05). Moreover, even slightly lengthened lifetime decay profiles of a possible donor component were observed in the HP11 film. The measured time constants of HPI in the film were 2.91 ns (57.3%) and 4.24 ns (42.7%) at 420 nm (χ^2 = 1.01). On the contrary, shortened lifetime decay profiles of *m*-MHPI obtained in both MP11 (1.39 and 2.81 ns at 420 nm) and MO11 (1.58 and 2.90 ns at 500 nm) films indicate the presence of energy transfer from *m*-MHPI to *p*-MHPIC and HPNO, respectively, consistent with the steady-state results stated above (see Supporting Information Figures S11–15 for decay profiles).

■ CONCLUSIONS

We have successfully constructed a molecular pixel system for full-color reproduction consisting of three primary color-emitting imidazole ESIPT molecules between which energy transfer was totally frustrated. The whole color gamut within the color triangle on the CIE 1931 diagram could be easily predicted and precisely reproduced by the simple mathematical operations based on additive color theory. It is expected that this unprecedented demonstration of molecular pixel system will pave the way to the innovative optoelectronic applications in future displays and biological imaging.

dx.doi.org/10.1021/ja404256s | J. Am. Chem. Soc. 2013, 135, 11239–11246

■ ASSOCIATED CONTENT

Supporting Information

Calculation details for mixing ratios and spectral overlap integrals, synthetic schemes, supporting figures, and lifetime decay profiles. This material is available free of charge via the Internet at http://pubs.acs.org.

■ AUTHOR INFORMATION

Corresponding Author

parksy@snu.ac.kr

Notes

The authors declare no competing financial interest.

■ ACKNOWLEDGMENTS

This research was supported by a National Research Foundation of Korea (NRF) grant funded by the Korea government (MSIP) (no. 2009-0081571).

■ REFERENCES

(1) Tang, C. W.; VanSlyke, S. A. *Appl. Phys. Lett.* **1987**, *51*, 913.
(2) Muller, C. D.; Falcou, A.; Reckefuss, N.; Rojahn, M.; Wiederhirn, V.; Rudati, P.; Frohne, H.; Nuyken, O.; Becker, H.; Meerholz, K. *Nature* **2003**, *421*, 829.
(3) Xiao, L.; Chen, Z.; Qu, B.; Luo, J.; Kong, S.; Gong, Q.; Kido, J. *Adv. Mater.* **2011**, *23*, 926.
(4) Wu, H. B.; Ying, L.; Yang, W.; Cao, Y. *Chem. Soc. Rev.* **2009**, *38*, 3391.
(5) Kamtekar, K. T.; Monkman, A. P.; Bryce, M. R. *Adv. Mater.* **2010**, *22*, 572.
(6) Farinola, G. M.; Ragni, R. *Chem. Soc. Rev.* **2011**, *40*, 3467.
(7) Valeur, B.; Leray, I. *Coord. Chem. Rev.* **2000**, *205*, 3.
(8) Johnsson, N.; Johnsson, K. *ACS Chem. Biol.* **2007**, *2*, 31.
(9) De, M.; Ghosh, P. S.; Rotello, V. M. *Adv. Mater.* **2008**, *20*, 4225.
(10) Yang, Y.; Zhao, Q.; Feng, W.; Li, F. *Chem. Rev.* **2012**, *113*, 192.
(11) Ohta, N.; Robertson, A. In *Colorimetry: Fundamentals and Applications*; Kriss, M. A., Ed.; The Wiley-IS&T Series in Imaging Science and Technology; John Wiley & Sons Ltd.: New York, 2005.
(12) Hunt, R. W. G. *The Reproduction of Colour*, 6th ed.; John Wiley & Sons: New York, 2004.
(13) Lakowicz, J. R. *Principles of Fluorescence Spectroscopy*, 3rd ed.; Springer: New York, 2006.
(14) Ajayaghosh, A.; Praveen, V. K.; Srinivasan, S.; Varghese, R. *Adv. Mater.* **2007**, *19*, 411.
(15) Shu, T. M.; Wu, J. C.; Lu, M.; Chen, L. Q.; Yi, T.; Li, F. Y.; Huang, C. H. *J. Mater. Chem.* **2008**, *18*, 886.
(16) Abbel, R.; van der Weegen, R.; Pisula, W.; Surin, M.; Leclere, P.; Lazzaroni, R.; Meijer, E. W.; Schenning, A. P. H. J. *Chem.-Eur. J.* **2009**, *15*, 9737.
(17) Vijayakumar, C.; Praveen, V. K.; Ajayaghosh, A. *Adv. Mater.* **2009**, *21*, 2059.
(18) Chen, Q.; Zhang, D.; Zhang, G.; Yang, X.; Feng, Y.; Fan, Q.; Zhu, D. *Adv. Funct. Mater.* **2010**, *20*, 3244.
(19) Giansante, C.; Raffy, G.; Schafer, C.; Rahma, H.; Kao, M. T.; Olive, A. G. L.; Del Guerzo, A. *J. Am. Chem. Soc.* **2011**, *133*, 316.
(20) He, G. J.; Guo, D.; He, C.; Zhang, X. L.; Zhao, X. W.; Duan, C. Y. *Angew. Chem., Int. Ed.* **2009**, *48*, 6132.
(21) Shiraishi, Y.; Ichimura, C.; Sumiya, S.; Hirai, T. *Chem.-Eur. J.* **2011**, *17*, 8324.
(22) Jayaramulu, K.; Kanoo, P.; George, S. J.; Maji, T. K. *Chem. Commun.* **2010**, *46*, 7906.
(23) Zhang, H.; Shan, X.; Zhou, L.; Lin, P.; Li, R.; Ma, E.; Guo, X.; Du, S. *J. Mater. Chem. C* **2013**, *1*, 888.
(24) Abbel, R.; van der Weegen, R.; Meijer, E. W.; Schenning, A. P. H. J. *Chem. Commun.* **2009**, 1697.
(25) Lei, Y. L.; Liao, Q.; Fu, H. B.; Yao, J. N. *J. Am. Chem. Soc.* **2010**, *132*, 1742.
(26) Tseng, K. P.; Fang, F. C.; Shyue, J. J.; Wong, K. T.; Raffy, G.; Del Guerzo, A.; Bassani, D. M. *Angew. Chem., Int. Ed.* **2011**, *50*, 7032.
(27) Balan, B.; Vijayakumar, C.; Ogi, S.; Takeuchi, M. *J. Mater. Chem.* **2012**, *22*, 11224.
(28) Liu, J.; Xie, Z. Y.; Cheng, Y. X.; Geng, Y. H.; Wang, L. X.; Jing, X. B.; Wang, F. S. *Adv. Mater.* **2007**, *19*, 531.
(29) Zhang, K.; Chen, Z.; Yang, C.; Tao, Y.; Zou, Y.; Qin, J.; Cao, Y. *J. Mater. Chem.* **2008**, *18*, 291.
(30) Park, M. J.; Kwak, J.; Lee, J.; Jung, I. H.; Kong, H.; Lee, C.; Hwang, D. H.; Shim, H. K. *Macromolecules* **2010**, *43*, 1379.
(31) Brovelli, S.; Sforazzini, G.; Serri, M.; Winroth, G.; Suzuki, K.; Meinardi, F.; Anderson, H. L.; Cacialli, F. *Adv. Funct. Mater.* **2012**, *22*, 4284.
(32) Baier, M. C.; Huber, J.; Mecking, S. *J. Am. Chem. Soc.* **2009**, *131*, 14267.
(33) Chen, J.; Zeng, F.; Wu, S. Z.; Su, J.; Tong, Z. *Small* **2009**, *5*, 970.
(34) Gao, H. F.; Poulsen, D. A.; Ma, B. W.; Unruh, D. A.; Zhao, X. Y.; Millstone, J. E.; Frechet, J. M. J. *Nano Lett.* **2010**, *10*, 1440.
(35) Wang, L.; Tan, W. H. *Nano Lett.* **2006**, *6*, 84.
(36) Melucci, M.; Zambianchi, M.; Barbarella, G.; Manet, I.; Montalti, M.; Bonacchi, S.; Rampazzo, E.; Rambaldi, D. C.; Zattoni, A.; Reschiglian, P. *J. Mater. Chem.* **2010**, *20*, 9903.
(37) Xu, J.; Liang, J.; Li, J.; Yang, W. *Langmuir* **2010**, *26*, 15722.
(38) Malinge, J.; Allain, C.; Brosseau, A.; Audebert, P. *Angew. Chem., Int. Ed.* **2012**, *51*, 8534.
(39) Abbel, R.; Grenier, C.; Pouderoijen, M. J.; Stouwdam, J. W.; Leclere, P. E. L. G.; Sijbesma, R. P.; Meijer, E. W.; Schenning, A. P. H. J. *J. Am. Chem. Soc.* **2009**, *131*, 833.
(40) Wild, A.; Teichler, A.; Ho, C.-L.; Wang, X.-Z.; Zhan, H.; Schlutter, F.; Winter, A.; Hager, M. D.; Wong, W.-Y.; Schubert, U. S. *J. Mater. Chem. C* **2013**, *1*, 1812.
(41) Kim, S.; Seo, J.; Jung, H. K.; Kim, J. J.; Park, S. Y. *Adv. Mater.* **2005**, *17*, 2077.
(42) Park, S.; Kwon, J. E.; Kim, S. H.; Seo, J.; Chung, K.; Park, S. Y.; Jang, D. J.; Medina, B. M.; Gierschner, J.; Park, S. Y. *J. Am. Chem. Soc.* **2009**, *131*, 14043.
(43) Sun, W. H.; Li, S. Y.; Hu, R.; Qian, Y.; Wang, S. Q.; Yang, G. Q. *J. Phys. Chem. A* **2009**, *113*, 5888.
(44) Kim, S. H.; Park, S.; Kwon, J. E.; Park, S. Y. *Adv. Funct. Mater.* **2011**, *21*, 644.
(45) Peng, H.-C.; Kang, C.-C.; Liang, M.-R.; Chen, C.-Y.; Demchenko, A.; Chen, C.-T.; Chou, P.-T. *ACS Appl. Mater. Interfaces* **2011**, *3*, 1713.
(46) Shono, H.; Ohkawa, T.; Tomoda, H.; Mutai, T.; Araki, K. *ACS Appl. Mater. Interfaces* **2011**, *3*, 654.
(47) Tang, K.-C.; Chang, M.-J.; Lin, T.-Y.; Pan, H.-A.; Fang, T.-C.; Chen, K.-Y.; Hung, W.-Y.; Hsu, Y.-H.; Chou, P.-T. *J. Am. Chem. Soc.* **2011**, *133*, 17738.
(48) Kwon, J. E.; Park, S. Y. *Adv. Mater.* **2011**, *23*, 3615.
(49) Zhao, J.; Ji, S.; Chen, Y.; Guo, H.; Yang, P. *Phys. Chem. Chem. Phys.* **2012**, *14*, 8803.
(50) Demchenko, A. P.; Tang, K.-C.; Chou, P.-T. *Chem. Soc. Rev.* **2013**, *42*, 1379.
(51) Frisch, M. J.; Trucks, G. W.; Schlegel, H. B.; Scuseria, G. E.; Robb, M. A.; Cheeseman, J. R.; Scalmani, G.; Barone, V.; Mennucci, B.; Petersson, G. A.; Nakatsuji, H.; Caricato, M.; Li, X.; Hratchian, H. P.; Izmaylov, A. F.; Bloino, J.; Zheng, G.; Sonnenberg, J. L.; Hada, M.; Ehara, M.; Toyota, K.; Fukuda, R.; Hasegawa, J.; Ishida, M.; Nakajima, T.; Honda, Y.; Kitao, O.; Nakai, H.; Vreven, T.; Montgomery, J. A., Jr.; Peralta, J. E.; Ogliaro, F.; Bearpark, M.; Heyd, J. J.; Brothers, E.; Kudin, K. N.; Staroverov, V. N.; Kobayashi, R.; Normand, J.; Raghavachari, K.; Rendell, A.; Burant, J. C.; Iyengar, S. S.; Tomasi, J.; Cossi, M.; Rega, N.; Millam, J. M.; Klene, M.; Knox, J. E.; Cross, J. B.; Bakken, V.; Adamo, C.; Jaramillo, J.; Gomperts, R.; Stratmann, R. E.; Yazyev, O.; Austin, A. J.; Cammi, R.; Pomelli, C.; Ochterski, J. W.; Martin, R. L.; Morokuma, K.; Zakrzewski, V. G.; Voth, G. A.; Salvador, P.; Dannenberg, J. J.; Dapprich, S.; Daniels, A. D.; Farkas, Ö.; Foresman, J. B.; Ortiz, J. V.; Cioslowski, J.; Fox, D. J. *Gaussian 09*, revision A.2; Gaussian, Inc.: Wallingford, CT, 2009.

(52) Lee, C.; Yang, W.; Parr, R. G. *Phys. Rev. B: Condens. Matter Mater. Phys.* **1988**, *37*, 785.
(53) Park, S.; Kwon, O. H.; Kim, S.; Park, S.; Choi, M. G.; Cha, M.; Park, S. Y.; Jang, D. J. *J. Am. Chem. Soc.* **2005**, *127*, 10070.
(54) Park, S.; Seo, J.; Kim, S. H.; Park, S. Y. *Adv. Funct. Mater.* **2008**, *18*, 726.
(55) Skonieczny, K.; Ciuciu, A. I.; Nichols, E. M.; Hugues, V.; Blanchard-Desce, M.; Flamigni, L.; Gryko, D. T. *J. Mater. Chem.* **2012**, *22*, 20649.
(56) Ciuciu, A. I.; Skonieczny, K.; Koszelewski, D.; Gryko, D. T.; Flamigni, L. *J. Phys. Chem. C* **2013**, *117*, 791.
(57) Nayak, M. K. *J. Photochem. Photobiol., A: Chem.* **2012**, *241*, 26.
(58) Mahajan, A.; Aulakh, R. K; Bedi, R. K; Kumar, S.; Kumar, S.; Aswal, D. K. *Synth. Met.* **2012**, *162*, 58.
(59) Park, S.; Kwon, J. E.; Park, S. Y. *Phys. Chem. Chem. Phys.* **2012**, *14*, 8878.
(60) Radziszewski, B. *Chem. Ber.* **1877**, *10*, 70.
(61) Voloshin, N. A.; Chernyshev, A. V.; Metelitsa, A. V.; Minkin, V. I. *Chem. Heterocycl. Compd.* **2011**, *47*, 865.
(62) Tang, C. W.; VanSlyke, S. A.; Chen, C. H. *J. Appl. Phys.* **1989**, *65*, 3610.
(63) See the Supporting Information.